Sensors and Materials, Vol. 37, No. 8 (2025) 3609–3620
MYU Tokyo

S & M 4140

Simulation of Noise Control of Elliptical Muffler in Smart Venting Flow-altering System

Tian-Syung Lan,[1] Min-Chie Chiu,[2*] Ho-Chih Cheng,[3] and Shih-Ming Cho[4]

[1]School of Artificial Intelligence, Guangzhou Huashang College,
No. 1, Huashang Road, Lihu Street, Zengcheng District, Guangzhou, Guangdong 511300, China
[2]Department of Mechanical and Materials Engineering, Tatung University,
No. 40, Sec. 3, Zhongshan N. Rd., Taipei City 10452, Taiwan
[3]Department of Intelligent Manufacturing Technology, Ling Tung University,
No. 1, Ling Tung Rd., Taichung City 40852, Taiwan
[4]Department of Computer Science and Engineering, Tatung University,
No. 40, Sec. 3, Zhongshan N. Rd., Taipei City 10452, Taiwan

(Received March 31, 2025; accepted July 31, 2025)

Keywords: finite element method (FEM), multi-inlet, elliptical, muffler, venting

Installing silencers in factories is crucial to the prevention of hearing damage caused by engine noise. For facilities with limited space, elliptical mufflers—known for their shape flexibility—are ideal. In real-world scenarios, factories often face multiple sources of intermittent venting noise. Traditionally, individual mufflers are installed at each noise source, which significantly increases manufacturing costs and consumes valuable site space. To address this issue cost-effectively and efficiently, in this study, we developed a smart venting flow-altering system, incorporating a single elliptical silencer with sensors, actuators, and a controller. The system intelligently directs venting flows into the muffler using a combination of solenoid valves, relays, microphones, a controller, and an advanced elliptical muffler design. The muffler incorporates multiple chambers, baffles, extended perforated/nonperforated tubes, sound-absorbing wool, and an eccentric inlet. A finite element method-based mathematical model was developed to predict the sound transmission loss of the system. To optimize noise reduction performance, several parameters were evaluated, including the diameter of the eccentric inlet, lengths of extended tubes, perforation ratios, muffler body length, elliptical axis dimensions, and acoustic flow impedance. This smart system offers a cost-effective and space-efficient solution to managing noise from multiple intermittent venting noise sources. The findings of this study provide valuable guidance for acoustic engineers seeking to tackle similar industrial noise challenges.

1. Introduction

Mufflers with acoustical wool have been widely used and researched for noise abatement.(1) Johnson *et al.* predicted the sound absorption coefficient on the basis of acoustical flow impedence, porosity, curvature, and viscous characteristics length.(2) Champoux and Allard

*Corresponding author: e-mail: mcchiu@gm.ttu.edu.tw
https://doi.org/10.18494/SAM5673

ISSN 0914-4935

advanced the method for the analysis of sound-absorbing properties using the thermal characteristics of sound.(3) Lafarge *et al.* established the Johnson–Champoux–Allard model to estimate the sound-absorbing coefficient.(4) Sullivan and Crocker researched how to increase acoustical performance using perforated tubes.(5) A series of theories and numerical techniques have been presented using coupled equations to address acoustical problems in using mufflers for noise abatement.(6–9) To understand the flow effect, Munjal(10) and Peat(11) proposed a generalized numerical decoupling method. Sathyanarayana and Munjal predicted the noise radiation of an engine exhaust system on the basis of a hybrid approach.(12) These previous research studies focused on a muffler with a simple geometrical shape. However, extensive studies of the acoustical effect from multiple noise sources based on the plane wave theory have not been conducted. Chiu and Chang conducted the acoustical simulation of a gun muffler inserted into an extended tube using the finite element method (FEM).(13) However, the acoustical performance of the muffler with an elliptical shape has not been studied sufficiently yet. To decrease the manufacturing cost of silencers and address noise from multiple sources, Lan *et al.* proposed a screw muffler with two inlets and one outlet.(14) They proposed a smart duct-switching system to effectively manage the air-flow path by controlling an electric valve and using a sound sensor.(14) To accommodate silencers installed in constrained spaces while maximizing acoustic performance, an elliptical-section muffler is required. Traditionally, in handling multiple intermittent venting noise sources, a dedicated muffler is used for each noisy venting source. However, from an economic standpoint, this approach leads to excessive costs in both manufacturing and land usage. To address these issues, in this study, we developed a smart venting flow-altering system that integrates a single elliptical-section muffler with sensors, actuators, and a controller. Each venting noise source is connected to the muffler via individual pipes (as illustrated in Fig. 1). To intelligently manage the venting flow, a microphone is installed in each pipe. The controller continuously monitors the sound levels from all pipes in real time. When an intermittent venting noise event occurs, the sound level detected by the microphone in the corresponding pipe exceeds a preset threshold. In response, the controller activates a relay system that triggers the solenoid valve in that pipe, opening the venting gate and directing the noisy airflow into the elliptical muffler for sound attenuation. This smart system offers an

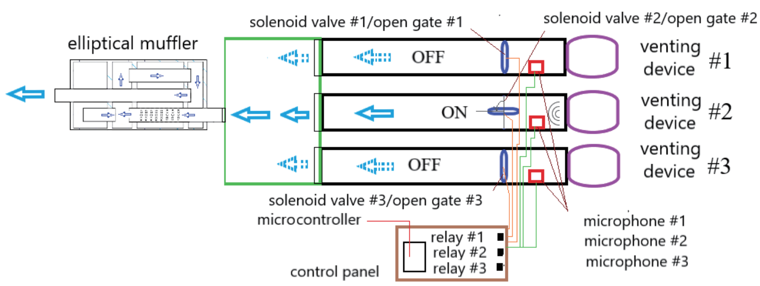

Fig. 1. (Color online) Schematic of a smart duct switching system used in dealing with the problem involving three sources of intermittent venting noise.

economical solution for noise reduction from multiple venting noise sources, simplifying installation and minimizing cost. The acoustic performance of the proposed system was evaluated using finite element modeling (via COMSOL Multiphysics), providing a foundation for the future development of efficient and cost-effective noise control solutions.

2. Structure of Smart Venting Flow-altering System

To demonstrate the smart system for handling multiple sources of intermittent venting noise, a scenario with three such sources is presented, and the schematic of the smart venting flow-altering system is shown in Fig. 1. As shown in Fig. 1, three microphones and three openable gates, each equipped with a solenoid valve, are installed on three separate pipes connected to their respective venting devices. These pipes direct venting noise into a shared tank, which has a single outlet connected to the elliptical muffler within the smart system.

3. Mathematical Model

An elliptical muffler, sound tubes, and an eccentric inlet are included in the system (Fig. 2). As shown in Fig. 2(a), to attenuate the sound wave energy around the perforated tube, the space between the pipes is filled with sound-absorbing wool.

COMSOL, a commercial package based on FEM, is used in the muffler's acoustical simulation. On the basis of a three-dimensional acoustical field, the boundary condition in the acoustical field used in the acoustical model in COMSOL is

$$n \cdot \left\{ \frac{1}{\rho_c} \left(\nabla p_t - q \right) \right\} = 0, \tag{1}$$

where ρ_c is the air density, q (preset to zero) is the dipole source, and c is the sound speed.

The boundary condition for the acoustical field of the tube in a solid boundary of the COMSOL model is described by Eqs. (2) and (3).

$$n \cdot \left\{ \frac{1}{\rho_c} \left(\nabla p_t - q \right) \right\} = -\left(p_{t1} - p_{t2} \right) \frac{i\omega}{Z_i} \tag{2}$$

$$Z_i = \rho_c c_c \left[\frac{1}{\sigma} \sqrt{\frac{8\mu k}{\rho_c c_c}} \left(1 + \frac{t_p}{d_h} \right) + \theta_f + i \frac{k}{\sigma} \left(t_p + \delta_h \right) \right] \tag{3}$$

The Johnson–Champoux–Allard model is used to analyze the acoustical behavior of porous acoustical wool in the system described by Eq. (4).

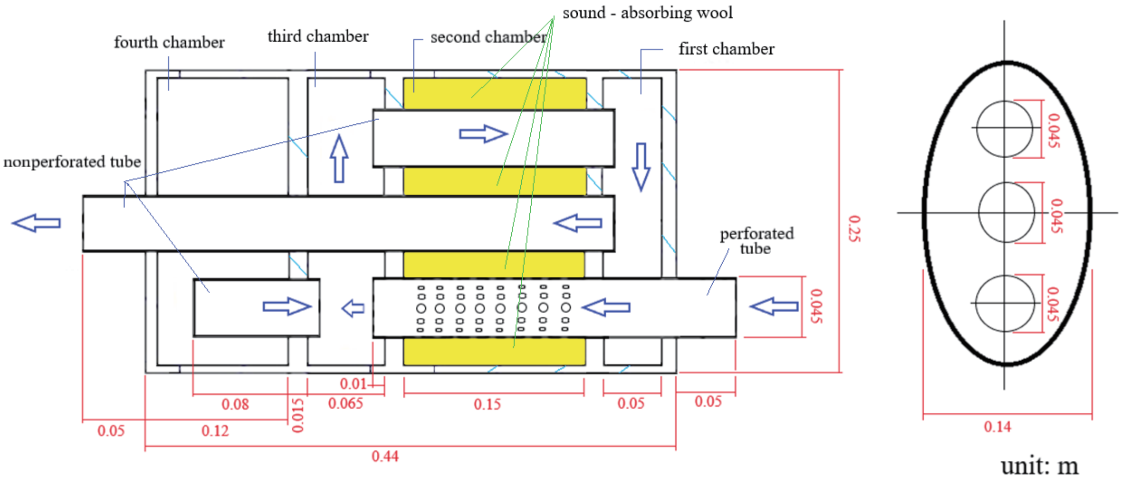

(a)

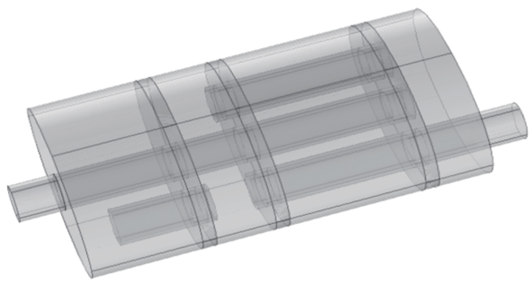

(b)

Fig. 2. (Color online) Elliptical muffler with extended tubes and eccentric inlet/outlet. (a) Two- and (b) three-dimensional sectional views.

$$\rho_{eff} = \alpha_\infty \rho_0 \left[1 + \frac{\sigma_0 \varphi}{j \rho_0 \omega \alpha_\infty} \left(1 + \frac{4 j \alpha_\infty^2 \eta \rho_0}{\sigma_0^2 \Lambda^2 \varphi^2} \right)^{1/2} \right], \tag{4}$$

where φ is the porosity of the material, σ_0 is the flow impedance, η is the curvature level, and α_∞, is the shearing viscosity.

The bulk factor (K_{eff}) is presented as

$$K_{eff} = \frac{\gamma P_0}{\gamma - (\gamma - 1) \left[1 + \frac{8\eta}{j \Lambda'^2 B^2 \omega \rho_0} \left(1 + j \rho_0 \frac{\omega B^2 \Lambda'^2}{16\eta} \right)^{0.5} \right]^{-1}}, \tag{5}$$

where Λ and Λ' are the viscous and thermal characteristic lengths, respectively. The governing equation of the sound wave propagating inside the muffler is

$$-\frac{1}{\rho_c}\left(\nabla p_t - q\right) - \frac{k_{eq}^2 p_t}{\rho_c} = Q, \tag{6a}$$

$$p_t = p + p_b;\ k_{eq}^2 = \left(\frac{\omega}{c_c}\right)^2;\ c_c = c;\ \rho_c = \rho. \tag{6b}$$

The sound transmission loss (TL) is defined as

$$TL = 10\log\frac{W_{in}}{W_{out}}. \tag{7}$$

The FEM model of the muffler with one chamber and extended tubes is established to calculate TL. The accuracies of the FEM (COMSOL package) models for the muffler with internally inserted perforated and nonperforated extended tubes are verified by the experimental data shown in Figs. 3 and 4.[15–17] The accuracy of the FEM (COMSOL package) model for the muffler filled with sound-absorbing wool is verified by the experimental data shown in Fig. 5.[17] The TLs calculated using the FEM (COMSOL package) model and the experimental data

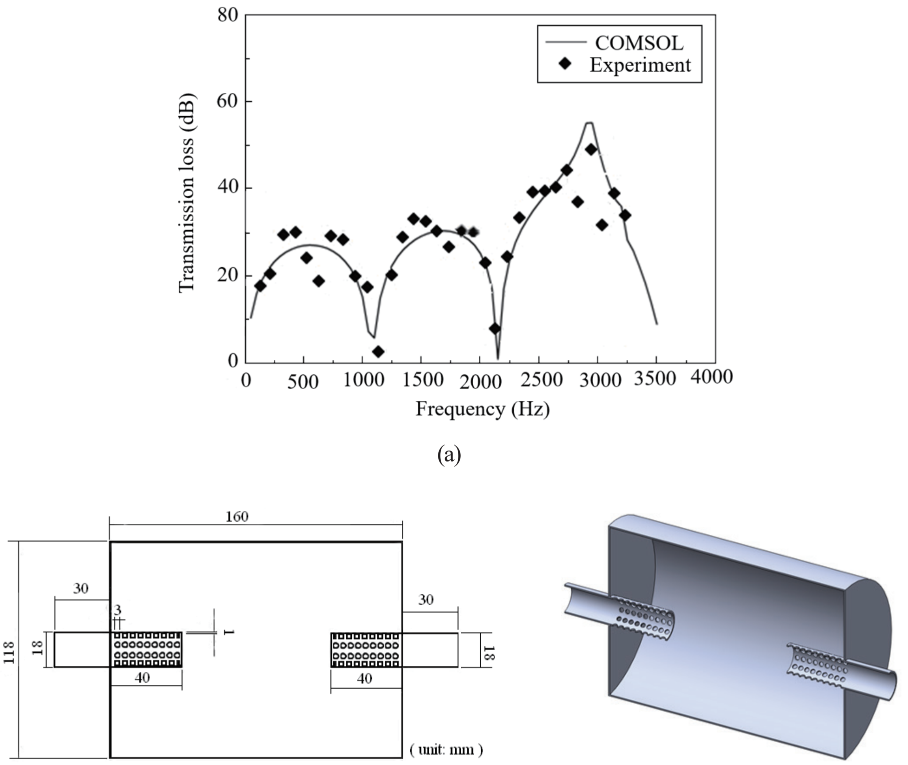

(a) (b) (c)

Fig. 3. (Color online) (a) TLs of muffler with one chamber and extended tubes and its structure [(b) and (c)].[13]

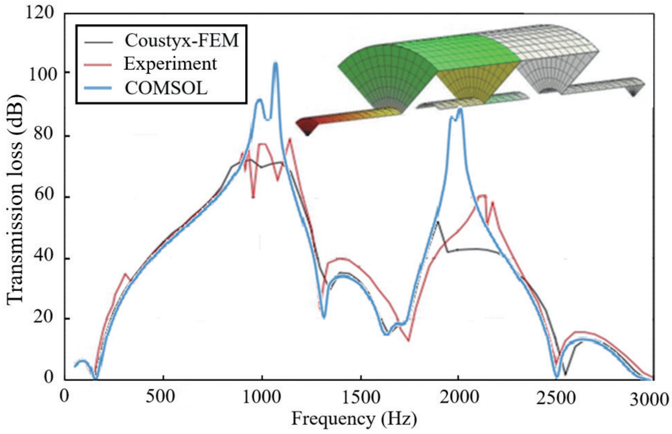

(a)

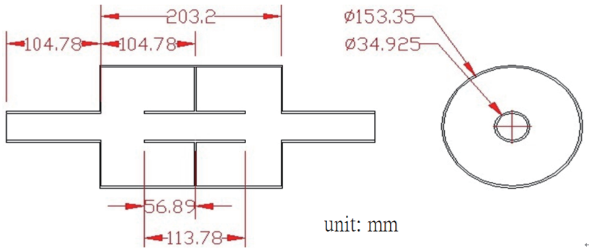

(b)

Fig. 4. (Color online) (a) *TL*s from Coustyx-FEM model, experimental data, and COMSOL model; (b) dimensions of muffler with extended tube.

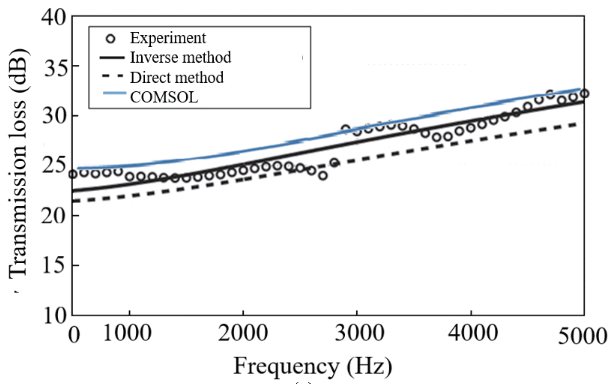

(a)

Diameter (D) [mm]	Thickness (H) [mm]	σ $[Pa \cdot s/m^2]$	ϕ [–]	$\alpha\infty$ [-]	Λ [μm]	Λ' [μm]
25.4	6.5	2.07E6	0.67	2.24	12.54	21.54

(b)

Fig. 5. (Color online) (a) *TL*s from experimental data, inverse method, direct method, and COMSOL model; (b) dimensions and properties of the sound-absorbing wool.[16]

coincided well (Fig. 3). The FEM model also shows similar *TL*s to the COMSOL model (Fig. 4). When including the sound-absorbing wool, the *TL*s of the FEM (COMSOL package) model and the experimental data also coincide well.

4. Results and Discussion

The results of simulation using the diameter of an eccentric inlet as a design parameter (Fig. 6) reveal that *TL* increases with the diameter of the eccentric inlet (Fig. 7). The different lengths of the first extended tube in the second and fourth chambers (Fig. 8) do not significantly affect *TL*, whereas the largest length (0.03 m) causes larger *TL*s and *TL* fluctuations at frequencies higher than 2000 Hz (Fig. 9). For different perforation ratios of the eccentric inlet in the third chamber (Fig. 10), the *TL*s and their fluctuations are similar (Fig. 11). *TL*s are similar for the total lengths of the muffler's body (0.41 and 0.44 m), whereas *TL*s for the length of 0.49 m are different from those for the different total lengths (Figs. 12 and 13). The lengths of the muffler's

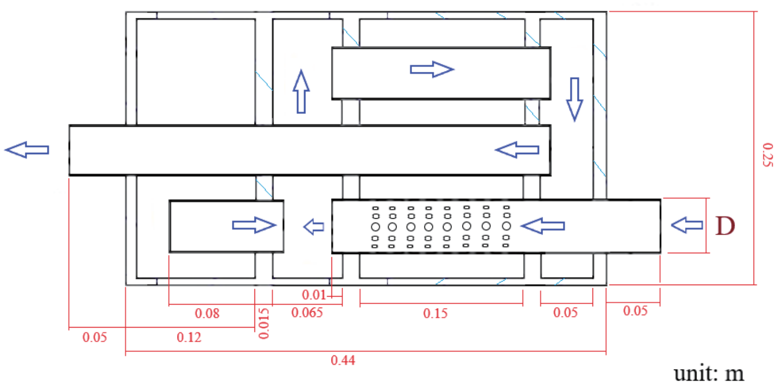

Fig. 6. (Color online) The selected parameter *D* (the diameter of an eccentric inlet).

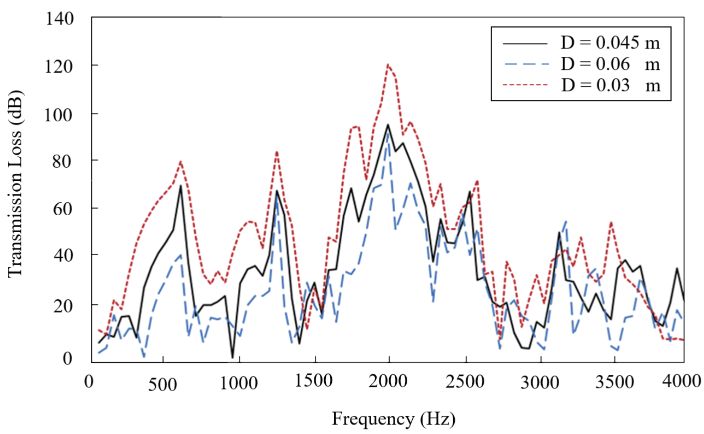

Fig. 7. (Color online) *TL* with respect to frequency at different *D*s.

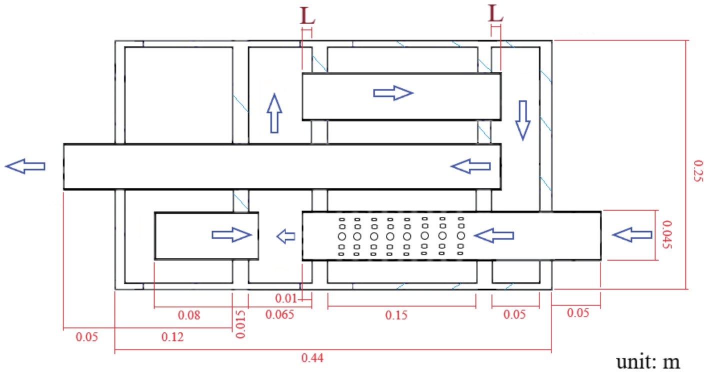

Fig. 8. (Color online) The selected parameter *L* (the lengths of the first extended tube in the second and fourth chambers).

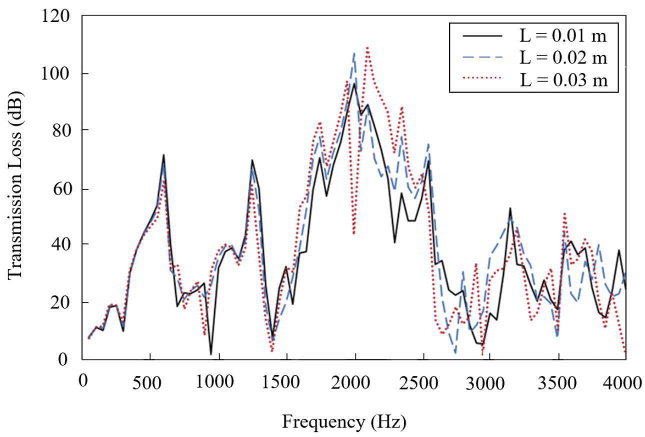

Fig. 9. (Color online) *TL* with respect to frequency at different *L*s.

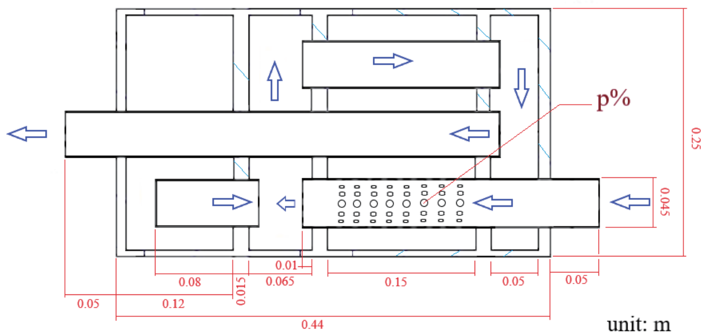

Fig. 10. (Color online) The selected parameter *P* (the perforation ratio of the eccentric inlet in the third chamber).

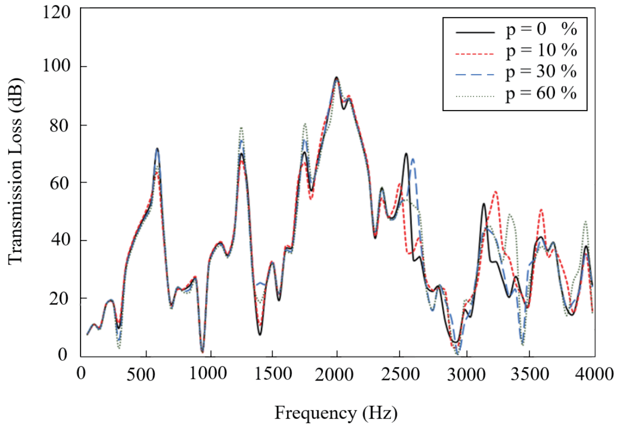

Fig. 11. (Color online) *TL* with respect to frequency at different *P*s.

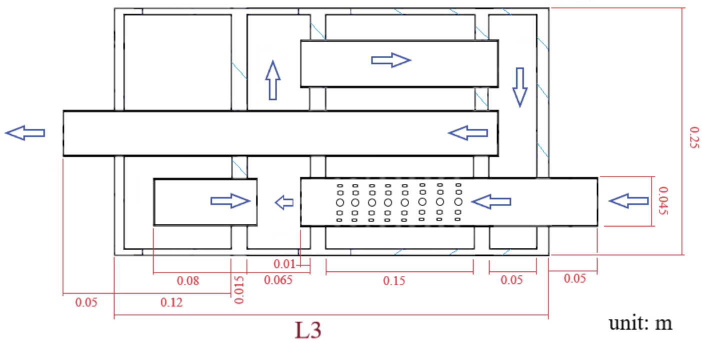

Fig. 12. (Color online) The selected parameter *L*3 (the length of the muffler's body).

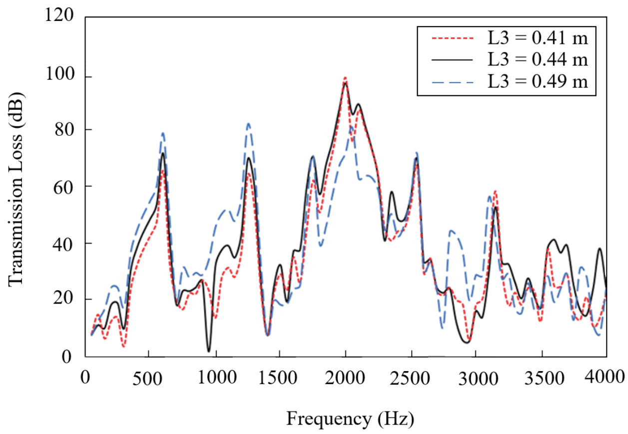

Fig. 13. (Color online) *TL* with respect to frequency at different values of *L*3.

axes affect *TL*s significantly. There is no specific trend of *TL* for different lengths of the axes (Figs. 14 and 15). The acoustical flow impedance of less than 10000 kg/m^3·s does not affect *TL* significantly. However, *TL* with the acoustical flow impedance of 10000 kg/m^3·s fluctuates more and becomes larger (Figs. 16 and 17).

The simulation and experiment results of *TL* show that *TL* is affected by various geometrical factors, including the diameter of an eccentric inlet, the lengths of the first extended tube in the second and fourth chambers, the perforation ratio of the eccentric inlet in the third chamber, the length of the muffler's body, the lengths of the two elliptical muffler's axes, and the acoustical flow impedance of the sound-absorbing wool. *TL* of the elliptical muffler increases when the acoustical flow impedance increases. The different values of the other parameters cause *TL*s to show different values. In general, the larger the values of the parameters, the larger the *TL* and its fluctuation. However, the different perforation ratios of the eccentric inlet in the third chamber do not cause significantly different *TL*s.

When addressing intermittent venting noise, the conventional approach of using a separate silencer for each noise source leads to high manufacturing costs and excessive use of space. To

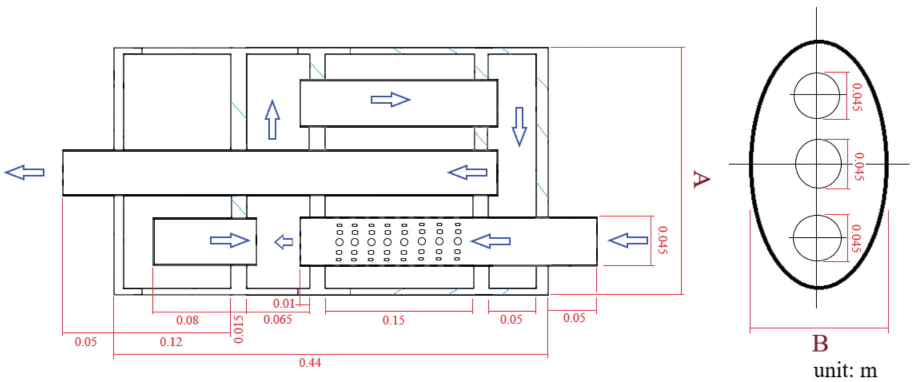

Fig. 14. (Color online) The selected parameters for *A* and *B* (the lengths of the muffler's axes).

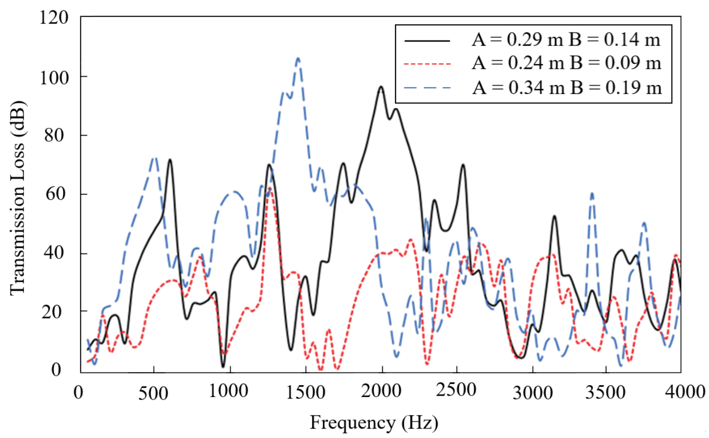

Fig. 15. (Color online) *TL* with respect to frequency at different parameter values of *A* and *B*.

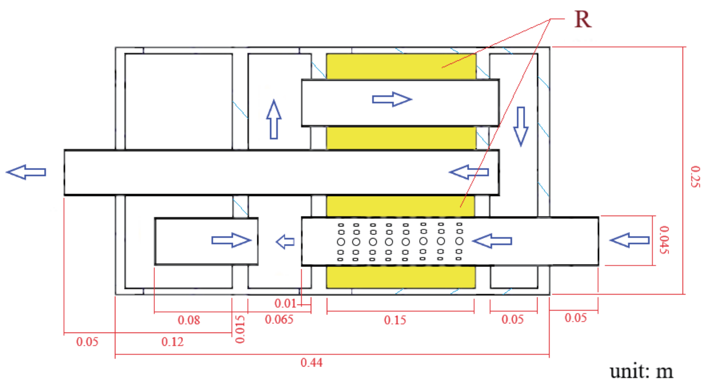

Fig. 16. (Color online) The selected parameter *R* (the acoustical flow impedance of the sound-absorbing wool).

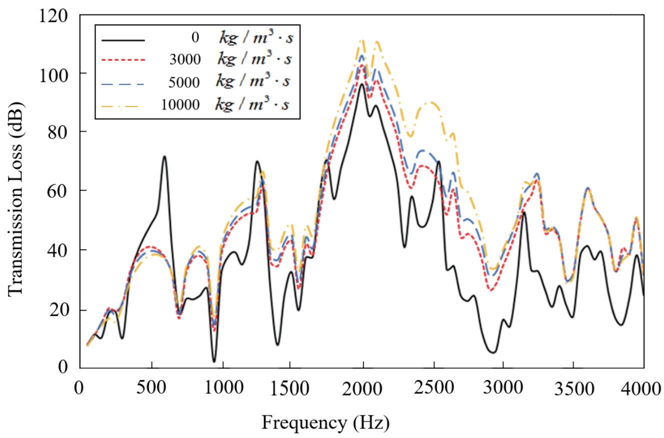

Fig. 17. (Color online) *TL* with respect to frequency at different *R*s.

effectively reduce these impacts, a smart system utilizing a single muffler is proposed. This system integrates solenoid valves with open gates, microphones, relays, a microcontroller, and one elliptical muffler. Each microphone monitors the noise level at its respective pipe. When the detected sound exceeds a predefined threshold—indicating venting—the microcontroller activates the corresponding solenoid valve via a relay system to open the gate, directing the noisy airflow into the muffler for attenuation. To facilitate installation in confined spaces, an elliptical muffler is selected owing to its shape flexibility, making it well-suited for the smart noise control system.

5. Conclusions

For facilities with limited space, elliptical mufflers—valued for their shape flexibility—are ideal. In practice, factories often contend with multiple sources of intermittent venting noise. Traditionally, separate mufflers are installed at each source, significantly increasing manufacturing costs and occupying valuable site space. To address these challenges cost-effectively and efficiently, in this study, we developed a smart venting flow-altering system that employs a single elliptical silencer along with sensors, actuators, and a controller.. The system intelligently routes venting flows into the muffler using solenoid valves, relays, microphones, a controller, and an advanced elliptical muffler design. To optimize noise attenuation, key parameters were analyzed, including the diameter of the eccentric inlet, extended tube lengths, perforation ratios, muffler body length, elliptical axis dimensions, and acoustic flow impedance. Simulation and experimental results indicate that *TL* is affected by multiple geometric parameters, including the diameter of an eccentric inlet, extended tube lengths, perforation ratios, muffler body length, elliptical axis lengths, and acoustical flow impedance. Generally, larger parameter values increase *TL* and its fluctuations, except for perforation ratios. Additionally, increased acoustical flow impedance enhances *TL*. Consequently, this smart system provides a cost-effective and space-efficient solution for managing noise from multiple intermittent venting noise sources. The findings of this study offer valuable insights for acoustic engineers facing similar industrial noise challenges.

References

1 M. E. Delany and E. N. Bazley: Appl. Acoust. **3** (1970) 105. https://doi.org/10.1016/0003-682X(70)90031-9
2 D. L. Johnson, J. Koplik, and R. Dashen: J. Fluid Mech. **176** (1987) 379. https://doi.org/10.1017/S0022112087000727
3 Y. Champoux and J. F. Allard: J. Appl. Phys. **70** (1991) 1975. https://ui.adsabs.harvard.edu/link_gateway/1991JAP....70.1975C/doi:10.1063/1.349482
4 D. Lafarge, P. Lemarinier, J. F. Allard, and V. Tarnow: JASA **102** (1997) 1995. https://doi.org/10.1121/1.419690
5 J. W. Sullivan and M. J. Crocker: Acoust. Soc. Am. **64** (1978) 207. https://doi.org/10.1121/1.381963
6 J. W. Sullivan: Acoust. Soc. Am. **66** (1979) 772. https://doi.org/10.1121/1.383680
7 K. Jayaraman and K. Yam: Acoust. Soc. Am. **69** (1981) 390. https://doi.org/10.1121/1.385465
8 P. T. Thawani and K. Jayaraman: Acoust. Soc. Am. **73** (1983) 1387. https://doi.org/10.1121/1.389245
9 M. L. Munjal, K. N. Rao, A. D. Sahasrabudhe: J. Sound Vib. **114** (1987) 173. https://doi.org/10.1016/S0022-460X(87)80146-3
10 M. L. Munjal: Acoustics of Ducts and Mufflers 2nd ed. (Wiley, Coshocton, 2014) Chap. 1.
11 K. S. Peat: J. Sound Vib. **123** (1988) 199. https://doi.org/10.1016/S0022-460X(88)80106-8
12 Y. Sathyanarayana and M. L. Munjal: Appl. Acoust. **60** (2000) 425. https://doi.org/10.1016/S0003-682X(00)00008-6
13 M. C. Chiu and Y. C. Chang: Noise Vib. Worldw. **54** (2023) 224. https://doi.org/10.1177/09574565231161651
14 T. S. Lan, M. C. Chiu, H. C. Cheng, and Y. D. Lin: Sens. Mater. **6** (2024) 2325. https://doi.org/10.18494/SAM4872
15 P. U. Hwang: Master degree, Taiwan University (2001). https://aleweb.ncl.edu.tw/F/GL8FSR96EXP5RDHFA4LKM2U111LQRPBSJ3HGKJRCF22S3EUJAL-15313?func=item-global&amp=&amp=&doc%5Flibrary=TOP02&doc%5Fnumber=001018721&pds_handle=GUEST
16 Coustyx software: http://coustyx.com/Products/Coustyx/Validation/Indirect/Muffler/Muffler-2/Downloads/dataset_description.pdf (accessed February 2025).
17 L. R. Barbosa and A. Lenzi: Appl. Acoust. **136** (2018) 94. https://doi.org/10.1016/j.apacoust.2018.02.019